Article

Neuroprotective effects of a novel demeclocycline derivative lacking antibiotic activity: from a hit to a promising lead compound

Rodrigo Tomas-Grau[1#], Florencia González-Lizárraga[1#], Diego Ploper[1], César L. Avila[1], Sergio B. Socías[1], Pierre Besnault[2], Aurore Tourville[2], Rosa M. Mella[3], Patricia Villacé Lozano[3], Clarisa Salado[3], Clémence Rose[4], Blandine Seon Méniel[4], Jean-Michel Brunel[5], Laurent Ferrié[4], Rita Raisman-Vozari[2], Patrick Pierre Michel[2], Bruno Figadère[4*], Rosana Chehín[1*]

[1] Instituto de Investigación en Medicina Molecular y Celular Aplicada (IMMCA) (CONICET-UNT-SIPROSA), Pasaje Dorrego 1080, 4000 San Miguel de Tucumán, Argentina; ro_tomasgrau@hotmail.com (R.T.G); mflorenciagl@hotmail.com.ar (F.G.L.); diegoploper@yahoo.com.ar (D.P.); cesar.avila@fbqf.unt.edu.ar (C.L.A.); sbsocias@yahoo.com.ar (S.B.S); rosana.chehin@fbqf.unt.edu.ar (R.C.)

[2] Paris Brain Institute, Inserm U 1127, CNRS UMR 7225, Sorbonne Université UM75, Paris, France; pierre.besnault@icm-institute.org (P.B.); aurore.tourville@icm-institute.org (A.T.); ritaraisman@gmail.com (R.R.V.); patrick.michel@icm-institute.org (P.M.)

[3] Innoprot SL, Parque Tecnológico de Bizkaia, Edificio 502 Planta 1 (48160) Derio, Spain; rmella@innoprot.com (R.M.L); pvillace@innoprot.com (P.V.L); csalado@innoprot.com (C.S.)

[4] BioCIS, Université Paris-Saclay, CNRS, 92290 Châtenay-Malabry, France; clemence.rose@live.fr (C.R.); blandine.seon-meniel@universite-paris-saclay.fr (B.S.M.); laurent.ferrie@universite-paris-saclay.fr (L.F.); bruno.figadere@u-psud.fr (B.F.).

[5] UMR_MD1 "Membranes et Cibles Thérapeutiques", U1261 INSERM, Aix-Marseille Université, 13385 Marseille; bruneljm@yahoo.fr (J.M.B).

# Rodrigo Tomás-Grau and Florencia González-Lizárraga have contributed equally to this work.

* Rosana Chehín, Pasaje Dorrego 1080, San Miguel de Tucumán, Tucumán-Argentina. Mail: rosana.chehin@fbqf.unt.edu.ar or Bruno Figadere 92290 Chatenay-Malabry, France. Mail: bruno.figadere@u-psud.fr.

Abstract: The antibiotic tetracycline demeclocycline (DMC) was recently reported to rescue α-synuclein (α-Syn) fibril-induced pathology. However, the antimicrobial activity of DMC precludes its potential use in long-term neuroprotective treatments. Here, we synthesized a DMC derivative with residual antibiotic activity and improved neuroprotective effects. The molecule, called derivative demeclocycline (DDMC), was obtained by the removal of both dimethylamino substituents at position 4 and the reduction of the hydroxyl group at position 12a on ring A of DMC. The modifications strongly diminished its antibiotic activity against Gram-positive and Gram-negative bacteria. Moreover, this compound preserved the low toxicity of DMC in dopaminergic cell lines while improving its ability to interfere with α-Syn amyloid-like aggregation, showing the highest effectiveness of all tetracyclines tested. Likewise, DDMC demonstrated the ability to reduce seeding induced by the exogenous addition of α-Syn preformed fibrils (α-Syn$_{PFF}$) in *ex vitro* models and in SH-SY5Y-α-SyntRFP cells. In addition, in the presence of DDMC, α-Syn$_{PFF}$ were less inflammogenic, as they dampened the release of tumor necrosis factor α (TNF-α) and glutamate by microglial cells compared to control fibrils. Our results suggest that DDMC may be a promising drug candidate for hit-to-lead development and preclinical studies in PD and other synucleinopathies.

Keywords: Parkinson's disease; novel tetracycline; neuroprotection

1. Introduction

In recent decades, tetracyclines (TCs) have been considered beyond their antibiotic effects. In fact, they have anti-inflammatory and anti-apoptotic activities and can exert a variety of biological actions, including the inhibition of proteolysis, angiogenesis, and tumor metastasis [1,2]. The pioneer work of Yrjanheikki and colleagues published in 1998 demonstrated that minocycline was neuroprotective in an animal model of ischemia [3].

Since then, more evidence has been reported, including a reduction in neuroinflammatory processes and the prevention of mitochondrial-mediated toxicity [4-9]. Moreover, it was recently reported that TC use in rosacea-treated patients was associated to a reduction in the risk of developing Parkinson's disease (PD) [10]. The neuroprotective effects of minocycline have also been described in PD animal models, where they are mainly attributed to the inhibition of microglial activation [11,12]. However, it seems that anti-inflammatory therapy *per se* is insufficient to account for neuroprotection, as PD patients in clinical trials being treated with minocycline showed no improvement [13].

Previously, we studied the ability of minocycline, doxycycline, and the non-antibiotic CMT-3 to interfere with α-Syn amyloid-like aggregation, since this process is widely considered to be central in triggering and spreading neurodegeneration in PD [14,15]. Our results demonstrated that dimethylamino (DMA) substituents, which are largely involved in antimicrobial activities [16], negatively correlate with neuroprotective qualities. In fact, minocycline, which possesses two DMA substituents located at C4 and C7, was incapable of inhibiting α-Syn aggregation and/or disrupting α-Syn preformed fibrils (α-Syn$_{PFF}$). Doxycycline, with only one DMA substituent at C4 interferes with aggregation but do not disassemble α-Syn$_{PFF}$. Finally, CMT-3, without any DMA substituent, is able to block α-Syn amyloid aggregation and even disassembled α-Syn$_{PFF}$ [17].

Recently, using a high-throughput drug discovery biosensor platform, demeclocycline (DMC) was selected from a 1280-compound small-molecule library (LOPAC) as a hit compound with enough potential to prevent neurodegeneration induced by the aggregation of α-Syn [18]. Interestingly, among 21 hit compounds identified by the biosensor, DMC showed the highest inhibition of αSyn-induced toxicity in the low nanomolar range (EC50 = 65 nM) and was tenfold more potent than previously described small molecules. Moreover, DMC efficiently rescued primary dopaminergic neurons from α-Syn$_{PFF}$-induced pathology. This data led to positioning DMC as an interesting compound for hit-to-lead optimization. However, the antibiotic activity of DMC strongly decreases its potential for long-term treatments, such as those required for PD and other synucleinopathies. A systematic revision of oral tetracycline administration during 2–18 weeks showed an increase in antibiotic resistance in subgingival, gastrointestinal, and upper respiratory tract flora [19]. It is relevant to consider that the frequency of microbial antibiotic resistance continues to increase and has emerged as one of the most critical problems in medicine.

Here, we aimed to advance the hit DMC compound towards a lead molecule with improved neuroprotective properties and minimal antibiotic activity, thus taking advantage of the neuroprotective potential of DMC while avoiding the antibiotic resistance dilemma. For this, we synthetized a new DMC derivative without any DMA substituents and reduced the hydroxyl group at position 12a on ring A of the molecule to obtain a novel non-antibiotic TC. The new molecule, named DDMC, showed only residual antibiotic activity, no toxicity in a dopaminergic cell model, and the ability to significantly diminish α-Syn amyloid-like aggregation at lower concentrations than previously tested TCs [17,20]. Furthermore, α-Syn$_{PFF}$ in the presence of the novel compound (α-Syn$_{PFF}$+DDMC) resulted in a significant reduction in proinflammatory factors released by primary microglial cell cultures. On the other hand, the fibrils formed in the presence of DDMC (α-Syn$_{PFF}$:DDMC) were less prone to induce aggregation and seeding in SH-SY5Y cells and were less inflammogenic than α-Syn$_{PFF}$. Taken together, these results position DDMC as a novel multimodal drug candidate as the lead molecule of the TC family with promising properties for preclinical and clinical studies in PD and other synucleinopathies.

2. Materials and Methods

2.1. -Synthesis of DDMC

In a 50mL round-bottom flask, demeclocycline hydrochloride (300 mg, 0.6 mmol, 1.0 eq) was suspended in AcOH (6.2 mL); then, zinc powder (391 mg, 6.02 mmol, 10 eq) was added and the reaction mixture was stirred for 20 h at room temperature. The resulting

solution was filtered through a small pad of Celite with AcOH. The organic phase was extracted with CH2Cl2, washed with HCl (1 M) and brine, dried over MgSO4, filtered off, and concentrated in vacuo. Precipitation in EtOAc/*n*-pentane produced compound 6 as a yellow solid (130.5 mg, 32%). Further purification was performed with preparative HPLC (XSelect 4.6x150 mm 5μm, H_2O+0.1%TFA: MeCN, 25:75 to 80:20 over 20 min. tr = 11.8 min).

¹H NMR (400 MHz, DMSO-*d6*): δ 18.45 (brs, 1H, OH), 14.71 (s, 1H, OH), 11.91 (s, 1H, OH), 9.11 (brs, 1H, NH), 8.72 (s, 1H, NH), 7.59 (d, *J* = 8.9 Hz, 1H), 6.95 (d, *J* = 8.9 Hz, 1H), 5.71 – 4.88 (brs, 1H, OH), 4.72 (d, *J* = 2.7 Hz, 1H), 3.68 (brs, 1H, CH_{12a}), 3.17 (brs, 1H, OH), 2.82 (ddd, *J* = 11.4, 5.6, 2.7 Hz, 1H), 2.46 – 2.55 (m, 3H), 1.87 (q, *J* = 12.2 Hz, 1H), 1.70 (ddd, *J* = 12.7, 5.6, 2.4 Hz, 1H) ppm. **¹³C{¹H NMR (100 MHz, DMSO-*d6*)**: δ ¹³C NMR (101 MHz, DMSO) δ 195.32, 191.73, 190.84, 177.76, 173.24, 160.12, 140.88, 136.60, 122.16, 118.72, 116.03, 104.33, 99.19, 63.91, 50.96, 37.97, 36.99, 29.05, 26.65 ppm.

HRMS: calculated for $C_{19}H_{17}ClNO_7$ [M+H]+ : 406.0688, found 406.0694.

2.2.-. *Expression and purification of human recombinant α-Syn*

Recombinant wild-type human α-synuclein was expressed in *Escherichia coli* using the pT7-7 plasmid encoding for the protein sequence. Purification was performed as previously described [21]. Protein purity was assessed using electrophoresis in polyacrylamide gels under denaturing conditions (SDS-PAGE). The stock solution of α-synuclein was prepared in 20 mM HEPES, 150 mM NaCl, pH 7.4. Prior to the aggregation assay, the protein stock solutions were centrifuged for 30 minutes at 12000 x *g* to remove microaggregates. Protein concentration was determined by measuring the absorbance at 280 nm using the extinction coefficient ε_{275} = 5600 cm⁻¹ M⁻¹.

2.3.-. *Antimicrobial assays*

The bacterial strains used in this study were *S. aureus* (ATCC25923), *E. coli* (ATCC25922), and *P. aeruginosa* (PA01). The strains were maintained at -80 °C in 15% (v/v) glycerol for cryoprotection. Bacteria were routinely grown in Mueller–Hinton (MH) broth at 37 °C.

The susceptibility of bacterial strains to antibiotics and compounds was determined in microplates using the standard broth dilution method in accordance with the recommendations of the Comité de l'Antibiogramme de la Société Française de Microbiologie (CA-SFM) [22]. Briefly, the minimal inhibitory concentrations (MICs) were determined with an inoculum of 10^5 CFU in 200 μL of MH broth containing two-fold serial dilutions of each drug. The MIC was defined as the lowest concentration of drug that completely inhibited visible growth after incubation for 18 h at 37 °C. To determine all MICs, the measurements were independently repeated in triplicate.

2.4. -*Cell viability assay*

Human neuroblastoma cell culture (SH-SY5Y) were grown in DMEM supplemented with 10% fetal bovine serum (FBS) and 1% penicillin/streptomycin (PS) at 37 °C and 5% CO2. For the cell viability assay, cells were seeded in 96-well plates at 15000 cells/well and maintained in 100 μl of DMEM supplemented with 2 % FBS and 1% PS for 24 h at 37 °C. Afterwards, the cells were treated with DMC or DDMC (10 or 50 μM final concentrations in each well). After treatment, they were incubated for 24 h at 37 °C and 5% CO2. To determine cell viability, a colorimetric MTT metabolic activity assay was used as previously described by Mosmann (Mosmann, 1983). All experiments were performed in sextuplicate, and the relative cell viability (%) was expressed as a percentage relative to the untreated control cells.

2.5. -*Protein aggregation assays*

The aggregation protocol was adapted from previous studies [17]. The different aggregated species were formed by incubating recombinant α-synuclein samples (70 μM) in

10 mM PBS, pH 7.4, in a Thermomixer Comfort® (Eppendorf) at 37 °C under orbital agitation at 600 rpm in the absence or presence of DMC or DDMC.

2.6. -Thioflavin T fluorescence assay

Aggregation studies with α-synuclein in the absence or presence of DMC or DDMC were performed by measuring the fluorescence emission of thioflavin T (ThT) at different time points according to LeVine [23][-70]. Changes in the emission fluorescence spectra were monitored at an excitation wavelength of 450 nm using an Fluoromax-4 spectrofluorometer.

2.7.-. Congo Red Absorbance Spectroscopy

A Congo red (CR) working solution was prepared prior to use by diluting the stock solution to reach a concentration of 10 mM in 10 mM PBS, pH 7.4. Fresh solution was prepared immediately before use. The samples used were obtained after the incubation of 70 μM α-Syn in the presence of DMC or DDMC. For absorbance measurements, the procedure was performed according to Medina et al., 2021 with minor adjustments. Each sample was mixed with PBS and CR solution to reach a final dye concentration of 20 μM. After that, a transparent 96-well plate was filled with 200 μl of each prepared sample, placed in a vortex, and mixed at 23 °C and 300 rpm for 30 min before being read in the same spectrometer. The absorption of each sample was recorded over a range of 400–700 nm using a TECAN Infinite M200 microplate reader. The CR absorbance was calculated according to the equation CRAb=(540Ab/25,295)- (475Ab/46,306), as previously described by Klunk et al. [24].

2.8. -Transmission electron microscopy (TEM)

Samples (50 μl) of a 70 μM α-Syn solution were adsorbed onto glow-discharged 200 mesh carbon film-coated copper grids (Electron Microscopy Sciences) and stained with uranyl acetate (2%). The excess liquid was removed, and the grids were allowed to air dry. The grids prepared in this way were analyzed using TEM. For TEM, the images were captured using a Philips 301 transmission electron microscope; for SEM, the images were taken at 3kV with a working distance between 3 and 3.8 mm and high vacuum using a ZEISS SUPRA FE-SEM microscope.

2.8. -In vitro protein seeding assay

Monomeric α-Syn solutions (70 μM) in 10 mM PBS, pH 7.4, were incubated in a Thermomixer comfort (Eppendorf) at 37 °C under orbital agitation at 600 rpm to form fibrils. After harvesting, the species were diluted 1/10 and further incubated with 70 μM of fresh monomers in the absence or presence of 10 μM DDMC. Aliquots were taken from the seeding aggregation at different times and mixed with the ThT probe, according to LeVine [25] . Changes in the emission fluorescence spectra (λ_{exc}= 450 nm) were monitored using a Horiba Fluoromax-4 fluorometer. Non-linear regression was used to fit the kinetic curves to a sigmoidal equation in GraphPad Prism, and the lag phases were calculated using the following equation: T50 – [1/(2*k)], where T50 is the time at which the fluorescence is halfway between the baseline and plateau values and k is the Hill slope according to Lau et al [26].

2.9. -Cell seeding assay

Recombinant human α -Syn (70 μM) was solubilized in 10 mM PBS (pH 7.4), filtered, centrifuged, and incubated for 120 h at 37°C under orbital agitation at 600 rev./min in a Thermomixer comfort (Eppendorf) to form fibrils. SH-SY5Y cells overexpressing the fusion protein α-Syn-tRFP were provided by Innoprot (Innoprot #P30707-02). These cells were plated on a 48-well plate at a density of 50,000 cells per well and either treated or not treated with 10 μM DDMC for 72 h with a 7 μg/ml suspension of α-Syn$_{PFF}$ aggregates. After treatment, the cells were fixed with 4% (wt/vol) paraformaldehyde (PFA) for 20 min at room temperature in the dark, followed by a permeabilization step with 0.1% (vol/vol)

Triton X-100 in PBS for 20 min at room temperature. The cells were finally stained with DAPI (1:5,000 in PBS) for 5 min and mounted on coverslips for confocal microscopy. Images were acquired with a ZEISS LSM800 confocal microscope at 63x and images analysis was performed using CellProfiler 4.2.1 [27]. Cell segmentation was performed with the RunCellPose plugin, while the granularity spectra of the cytoplasm was evaluated with the granularity module.

2.10. -Immunofluorescence and lysosome identification

For studying lysosomes, SH-SY5Y cells were grown to 80% confluency in 24-well plates on round coverslips which were previously washed with ethanol, PBS buffer, and culture medium. After O/N incubation with or without DDMC, LysoTracker™ Deep Red (Invitrogen #L12492), diluted 1:1,000 in prewarmed medium, was added to the SH-SY5Y cells for 5 min at 37°C and 5% CO_2. Afterwards, the cells were washed three times with warm media and fixed with fresh 4% (wt/vol) paraformaldehyde (PFA) diluted in PBS for 20 min at room temperature protected from light. After this, they were washed for 10 min three times in freshly prepared PBS and mounted for microscopy. For immunostaining LAMP1-positive vesicles, SH-SY5Y cells were also grown on coverslips in similar conditions to those described above and treated or not treated with DDMC followed by O/N incubation. The next day, the cells were fixed in fresh PFA for 20 min, washed for 10 min three times in freshly prepared PBS, permeabilized by treatment with 0.2% (vol/vol) Triton X-100 in PBS for 10 min, and washed again for 10 min three times with PBS. The samples were then blocked with 5% dry milk and 0.5% BSA in PBS (blocking solution) for 2 h. Immunofluorescence was performed with rabbit monoclonal anti-LAMP1 primary antibodies (Cell Signaling #3243S) at a dilution of 1/300 in a solution of 1/10 blocking solution in PBS and incubated overnight at 4°C. The following day, the wells were washed for 10 min three times with PBS, and goat anti-rabbit IgG (H+L) cross-adsorbed to Alexa Fluor 488 secondary antibodies (Invitrogen #A11008) at a 1/750 dilution (also diluted in 1:10 blocking solution) and applied for 2 h at room temperature in the dark, followed by a wash step with PBS for 10 min three times. For both, the LysoTracker™ and immunostaining of LAMP1, cell nuclei were stained before mounting with DAPI for 5 minutes and washed three times with PBS. The coverslips were then mounted on microscopy slides with 4 μl of Vectashield Antifade Mounting Media (Vector Laboratories #H1000). The samples were visualized and analyzed with a ZEISS LSM800 confocal microscope at 63x magnification. Image analysis for lysosome quantification was performed with the granularity module in CellProfiler 4.2.1 [27].

2.11. -Primary microglial cell treatments

Microglial cell isolation: A coating procedure was performed as described previously [28]. Briefly, polycation coating solutions containing 1 mg/ml polyethyleimine (PEI) were applied to culture vessels for 2 h at 37ºC then, they were washed with PBS and used for cell seeding. Newborn mice were sacrificed and had their brains rapidly dissected. Two mouse brains were plated onto PEI-coated Corning T-75 flasks (Sigma-Aldrich) with 12 ml of complete medium (DMEM + 10% FBS and antibiotics) and incubated at 37ºC in an atmosphere of 95% air and 5% CO_2. A total of 10 ml of the culture medium was removed 48 h after plating to eliminate floating debris, and 10 ml of fresh medium was added. No additional medium was added until the total disappearance of other cell types. To produce subcultures, microglial cells were recovered by trypsin proteolysis using an EDTA (2 mM)-trypsin (0.05 %) solution and seeded onto non-coated Nunc 96-well plaques at a density of 20000 cells per well for 24 h using N5B medium (N5 medium + 5% HS + 0.5% FBS + 5 μM glucose) with 100 μM glycine.

α-Syn preparation for microglial cell treatments: To obtain α-Syn$_{PFF}$ from the monomeric recombinant α-Syn after the aggregation assay, the endotoxins were removed. We used a high-capacity endotoxin removal spin column (ThermoFisher, #88274) following the manufacturer's instructions. Then, protein samples were filtered through a 0.21 μm diameter pore membrane and centrifuged for 30 min at 12000 × g, and all residual

endotoxins were quantified using a Limulus Amebocyte Lysate chromogenic endotoxin quantification kit (ThermoFisher, #88288). Monomeric α-Syn stock solutions containing less than 1.2 endotoxin units (EU)/ml were used to obtain α-Syn$_{PFF}$ or α-S$_{PFF}$:DDMC following the same aggregation conditions described above. Before treating microglia cells, the aggregates were sonicated with a sonicator for 10 cycles at high power (30 s on and 30 s off, at 10 °C).

Dialysis*:* The samples tested in primary cell cultures were dialyzed twice against 10 mM PBS, pH 7.2, for 24 h using Slide-A-Lyzer™ 10 k Dialysis Cassettes (ThermoFisher, #66380). DDMC removal from samples was confirmed using spectroscopic methods.

2.12. -Statistical analysis

For the ThT fluorescence assay, Congo red absorbance spectroscopy, and *ex vitro* and in cell model protein seeding assay, statistical analyses were performed using one-way ANOVA, *t* test and Kruskal-Wallis test.

3. Results

3.1-. Non-antibiotic and non-toxic tetracycline obtained by chemical modifications of DMC

In order to eliminate the characteristic antibiotic activity of tetracyclines, DMC was subjected to chemical modifications. The removal of the DMA substituents at position 4 of the A ring, which are mainly responsible for the antimicrobial activity of tetracyclines [16], was performed in a one-step reaction, as shown in Figure 1a. As previously reported, DMC was treated with zinc in acetic acid and water for 2 h at room temperature [29-31]. After purification with preparative HPLC, the NMR data obtained from the compound, revealed the complete structure of the molecule, which we named DDMC. Surprisingly, in addition to the efficient removal of the DMA group, the reaction also caused the reduction of the hydroxyl group at position 12a. It is important to note that these chemical modifications did not affect the region that was previously attributed to binding aggregated α-Syn species [32].

The above products (DDMC and DMC) were evaluated for their antimicrobial activities against both Gram-negative (*Pseudomonas aeruginosa* PA01 and *Escherichia coli* ATCC 25922) and Gram-positive bacteria (*Staphylococcus aureus* ATCC 25923). As a general trend, DMC exhibited the most pronounced activity against these bacteria with minimum inhibitory concentrations (MICs) of 6.25 µM, 3.125 µM, and 0.4 µM, respectively (Figure 1b). As expected, with the removal of the DMA group, DDMC presented only residual antibiotic activities against Gram-negative bacteria while showing a 30-fold reduction in antibiotic activity against Gram-positive bacteria (MIC of 12.5 µM), with respect to that obtained for other TCs [33] (Figure 1b).

DMC is clinically used to treat susceptible bacterial infections and can be systemically administrated due to its low toxicity in human cells, even neurons [34]. In order to uncover if this was also the case for DDMC, we first evaluated its impact on cell viability by measuring MTT turnover [35] in SH-SY5Y cell cultures, using similar concentrations as those shown in Braun et al. for DMC [18]. The results showed no statistical differences between both compounds, tested at 10 and 50 µM, with respect to the control conditions (Figure 1c). This finding allowed us to use both concentrations to study the neuroprotective properties of DDMC.

Given that dysfunctions in the lysosomal pathway have been proved to be a key player in neurodegenerative diseases [36,37], we used LysoTracker™ Deep Red to test if DDMC could affect these organelles. This dye accumulates specifically in acidic vesicles and is widely used for determining the number and location of lysosomes [38]. As shown in Figure 1d, the overnight (O/N) treatment of SH-SY5Y-α-Syn-tRFP cells with 10 µM of DDMC did not induce any changes in the number or intensity of LysoTracker™-positive puncta. We also assayed the pan-lysosomal marker lysosomal-associated membrane protein 1 (LAMP1) [38] using immunofluorescence. As has been shown previously by others, the untreated SH-SY5Y- α-Syn-tRFP cells displayed abundant LAMP-1-positive vesicles (Figure 1d) [39]. Again, after an O/N treatment with DDMC, no significant differences

were observed compared to the untreated samples, suggesting that this compound does not affect the number or distribution of lysosomes, which represent a crucial clearance mechanism for the protein aggregates that are thought to trigger neurodegenerative diseases [36,37].
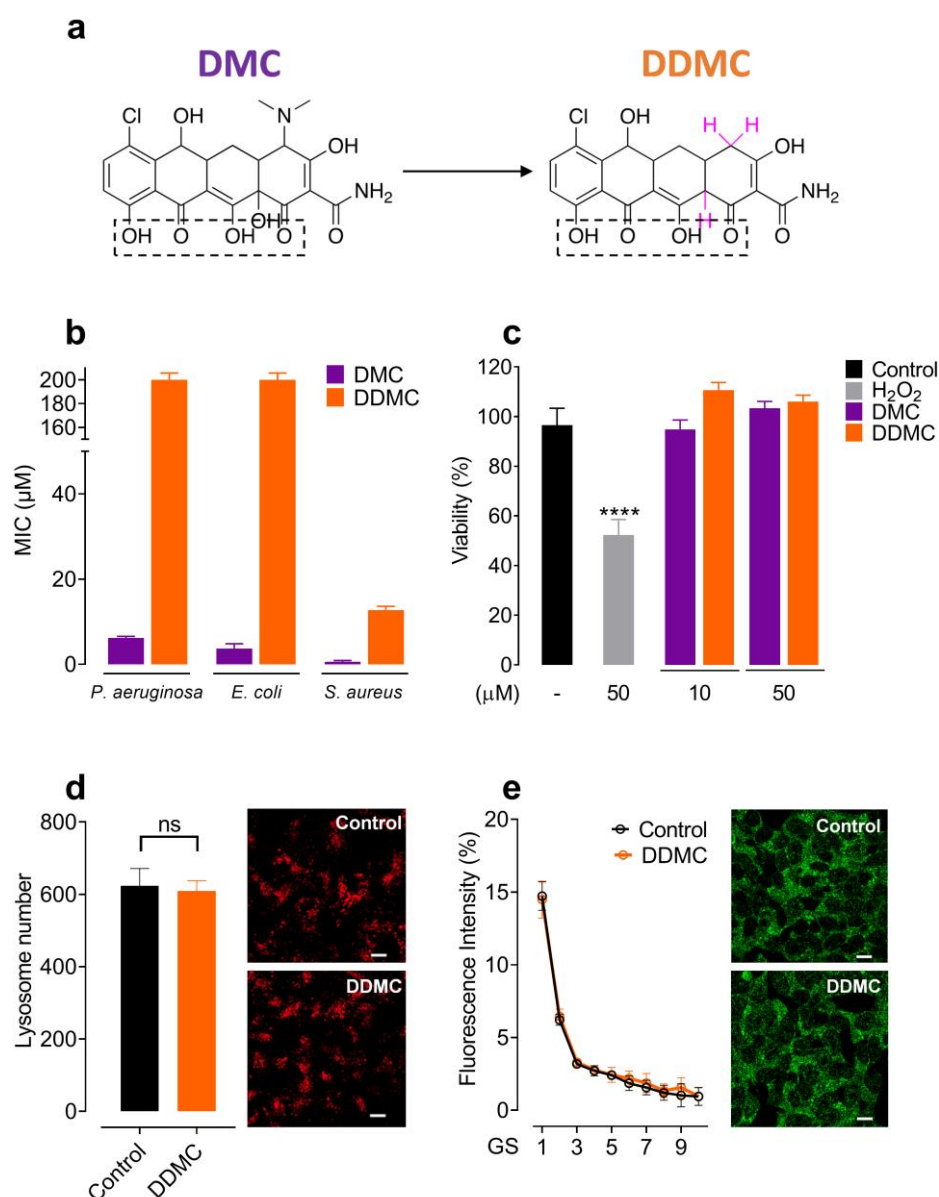

Figure 1. The novel TC DDMC is innocuous in bacteria and human cells. (**a**) Synthesis of reduced demeclocycline (DDMC) via the treatment of demeclocycline (DMC) with zinc in acetic acid and water for 2 h at room temperature. The hydrogen atoms incorporated due to the reduction step, and in the dashed-line box is the structural signature related to binding with amyloid-like aggregates. (**b**) Antibiotic activities of DMC and DDMC against *P. aeruginosa* (PAO1), *E. coli* (ATCC 25922), and *S. aureus* (ATCC 25923). MIC results are shown with the concentrations in μM in brackets. (**c**) MTT cell viability assay in SH-SY5Y cells after 24 h treatment with DMC or DDMC (10 or 50 μM final concentrations) and hydrogen peroxide (H_2O_2) as a positive control (50 μM). All experiments were performed in sextuplicate, and relative cell viability was expressed as a percentage relative to the untreated control cells (%). Statistical analysis was performed as described in Materials and Methods, and significant differences are indicated in the figures as follows: **** $p < 0.001$ vs. control; ns— $p > 0.05$ vs. control. (**d**) The effect of 10 μM DDMC on lysosome numbers was assessed using LysoTracker™ Deep Red staining in SH-SY5Y cells and confocal microscopy. (**e**) The number of LAMP1-positive vesicles was estimated using immunostaining and captured with a confocal

microscope. Lysosome quantification for (**c**) and (**d**) was performed with the granularity module in CellProfiler 4.2.1 [27].

3.2-. Comparative effect of DMC and DDMC on the inhibition of α-Syn aggregation

The ability of DMC to interfere with α-Syn amyloid-like aggregation has been previously reported [18]; however, its antibiotic activity would hinder its repositioning as a neuroprotector. To study if DDMC retained the antiaggregant property shown by its precursor DMC, we monitored the ability of both TCs to inhibit α-Syn self-assembly. For this, 70 μM of fresh α-Syn protein was incubated in the absence or presence of 10 and 50 μM of each TC. The cross-β structure, which is the hallmark of amyloid aggregation [40], was monitored by thioflavin T (ThT) fluorescence emission at 482 nm (λ_{exc} 450 nm) [23].

In the presence of 50 μM DMC, the ThT fluorescence intensity—as expected—decreased by around 75% (p< 0.0001) compared to the control, while the effect at 10 μM was significantly less pronounced (26%, p= 0.0148) (Figure 2a). Surprisingly, DDMC was more effective than its precursor; at 50 μM, the ThT signal was almost completely abolished (p< 0.0001). Moreover, at 10 μM, DDMC remained capable of inhibiting α-Syn cross-β formation, reaching a significant ThT signal reduction of 65% (p< 0.0001) (Figure 2a). These data strongly suggest that the chemical modifications introduced to DMC improved the ability of DDMC to interfere with α-Syn amyloid-like aggregation,

The binding mode(s) of molecular dyes for amyloid fibrils is not fully understood. However, there is some consensus that ThT binds inside channels running parallel to the long axis of the fibril [41], while Congo red (CR), binds in grooves formed along the β-structure [42]. Therefore, both assays are complementary and when used together provide deeper information on amyloid formation. Consequently, we complemented our results by studying the bathochromic shift in CR absorbance [24,43]. As shown in Fig 2b, DDMC (10 μM, the lower concentration tested before) diminished the CR signal by 43% (p< 0.0001) with respect to the control, while DMC showed no significant spectral difference (p= 0.0735). Although the red shift in CR lacks sensitivity compared to ThT at low amyloid fibril concentrations [25], the results obtained in Figure 2b agree with the ThT fluorescence depicted in Figure 2a.

To confirm these results, we resorted to transmission electron microscopy (TEM) to visualize the effects of DMC and DDMC on α-Syn aggregation. Figure 2c shows that DMC and DDMC both interfered with fibril formation. However, the reduction in fibrillar species formed in the samples incubated with DDMC compared to those treated with DMC was consistent with the decrease in cross-β structures depicted in Figure 2a. From these results, we concluded that DDMC was more potent than DMC at inhibiting α-Syn amyloid-like aggregation.
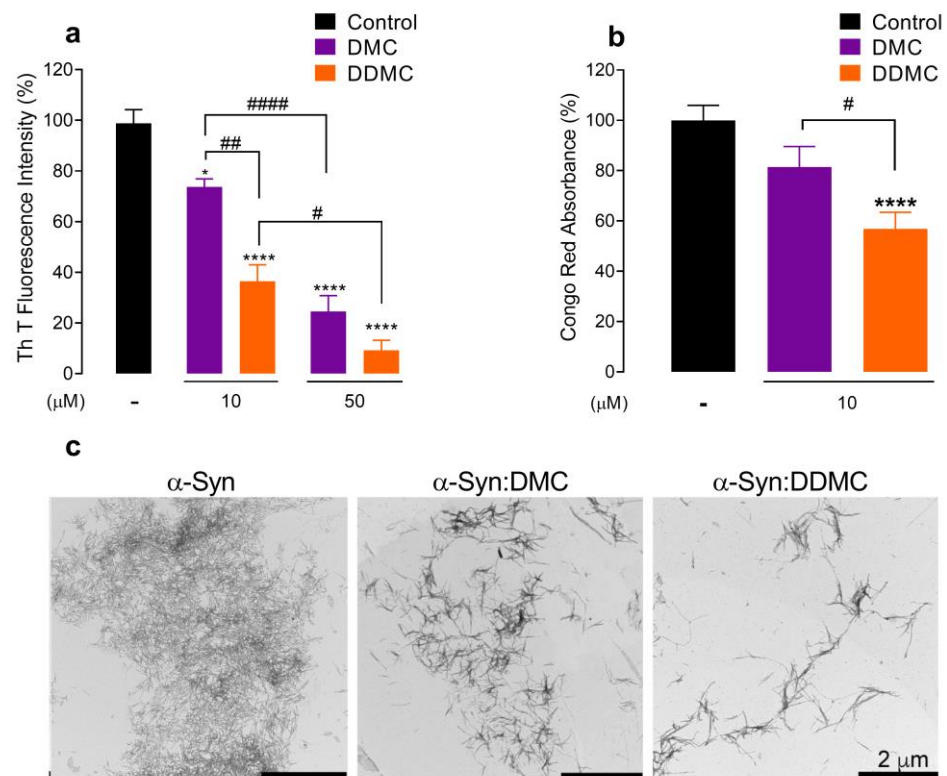
Figure 2. Comparative effect of DMC and DDMC on the inhibition of α-Syn aggregation. (**a**) Effect of DMC and DDMC on α-Syn aggregation as measured by the fluorescence emission intensity of 25 μM ThT in a solution containing 70 μM α-Syn incubated in the presence of 10 or 50 μM DMC or DDMC, after 120 h of incubation. (**b**) Absorbance of 20 μM Congo red in a solution containing 70 μM α-Syn incubated in the presence or absence of 10 μM DMC or DDMC. Values represent the mean + - SEM, and statistical analyses were performed as described in Materials and Methods. Significant differences are denoted with *. Comparisons between two groups were performed with a t-test (n= 5) with significant differences are denoted by #. (**c**) Transmission electron microscopy (TEM) of α-Syn samples incubated for 120 h in the presence of 10 μM DMC or DDMC.

3.3-. Effect of DDMC on α-Syn preformed fibril seeding activity

According to the nucleation/polymerization model, preformed α-Syn fibrillar species (α-Syn$_{PFF}$) have the ability to induce and accelerate the aggregation of the soluble monomeric protein and could be considered as seeds in this reaction [44]. To assess the ability of DDMC to inhibit the seeding competence of α-Syn$_{PFF}$, we compared the aggregation kinetics of monomeric α-Syn (α-Syn$_m$) to α-Syn$_m$ seeded with α-Syn$_{PFF}$ in the absence (α-Syn$_m$+α-Syn$_{PFF}$) or presence of 10 μM DDMC (α-Syn$_m$+α-Syn$_{PFF}$+DDMC). As shown in Figure 3a, the α-Syn amyloid-like fibril formation kinetics displayed a typical sigmoidal curve. In fact, we observed a 15 h lag phase followed by exponential growth that finally reached a plateau at 48 h, as was previously described in [14]. The addition of α-Syn$_{PFF}$ to the α-Syn$_m$ solution accelerated the aggregation process, with kinetics that were fit to a hyperbolic function (Figure 3a). Surprisingly, the presence of DDMC at the beginning of the aggregation process caused a significant decrease in ThT fluorescent intensity at all time points evaluated (Figure 3a), and a 6 h lag phase appeared (Figure 3b).
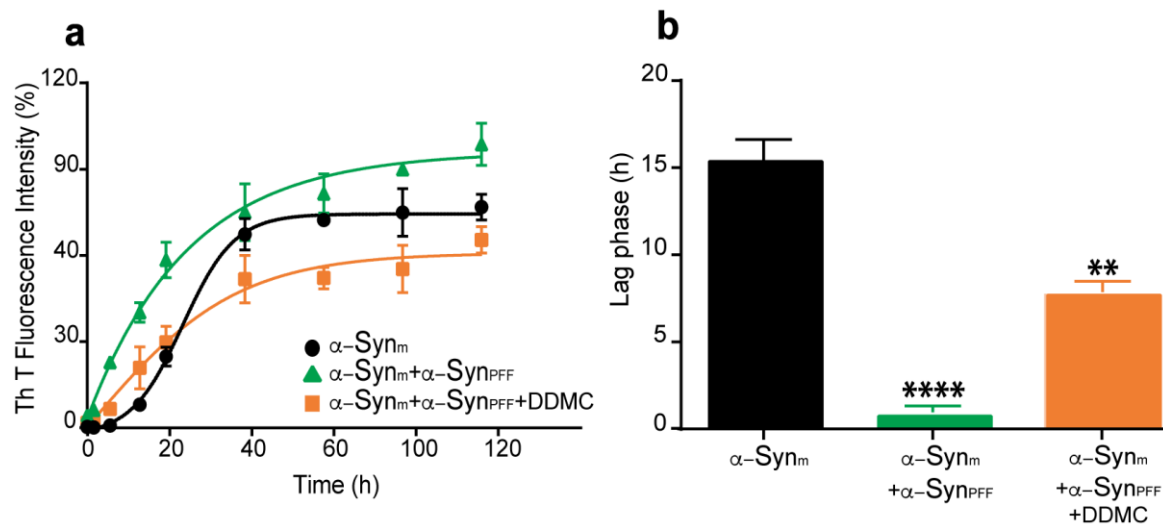
Figure 3. Effect of DDMC on α-Syn seeding induced by externally added α-Syn$_{PFF}$. (**a**) Fluorescence emission intensity of 25 μM ThT in a solution containing 70 μM monomeric α-Syn (α-Syn$_m$) alone (black circles) or seeded with α-Syn$_{PFF}$ (α-Syn$_m$+α-Syn$_{PFF}$) in the absence (green triangles) or presence of DDMC (α-Syn$_m$+α-Syn$_{PFF}$+DDMC) (orange squares) after 120 h of incubation. For each time point, values represent the mean + SEM. (**b**) Lag phase quantification based on the kinetics of aggregation of the seeding assay as described in Materials and Methods. Statistical significance is indicated as: ****$p< 0.01$; **$p< 0.01$ vs α-Syn$_m$.

3.4-. Effect of DDMC on the exogenous α-Syn$_{PFF}$-induced seeding of cytoplasmatic α-Syn

Despite the fact that α-Syn$_{PFF}$ formed from soluble α-Syn$_m$ differ at the atomic level from those recovered from the brains of PD patients [45], these species can seed the aggregation of endogenous α-Syn in different models, including cultured neuronal cells, primary cultured neurons, and animal brains [46-49]. Considering the ability of DDMC to inhibit the seeding competence of α-Syn$_{PFF}$, we complemented our biophysical studies with a dopaminergic cell model. For this, we used an SH-SY5Y transgenic cell line that constitutively overexpresses α-Syn fused to tRFP (Innoprot #P30707-02). In the absence of α-Syn$_{PFF}$, the fusion protein was expressed in most cells with a diffuse and faint cytoplasmic pattern (Fig 4a). On the contrary, the addition of exogenous α-Syn$_{PFF}$ induced the formation of intense α-Syn-tRFP puncta, which strongly resembled α-Syn aggregates (Figure 4b) [50,51]. However, when α-Syn$_{PFF}$ were added together with 10 μM DDMC, these puncta were diminished (Fig 4c). The quantification of these tRFP-positive puncta, expressed as granularity (described in Materials and Methods), showed a significant increase from 0.46 to 0.63 after α-Syn$_{PFF}$ addition; in cells treated with α-Syn$_{PFF}$+DDMC, the values were significantly reduced to the levels shown in the control cells. These results suggested that the seeding competence of α-Syn$_{PFF}$ was efficiently inhibited by DDMC.
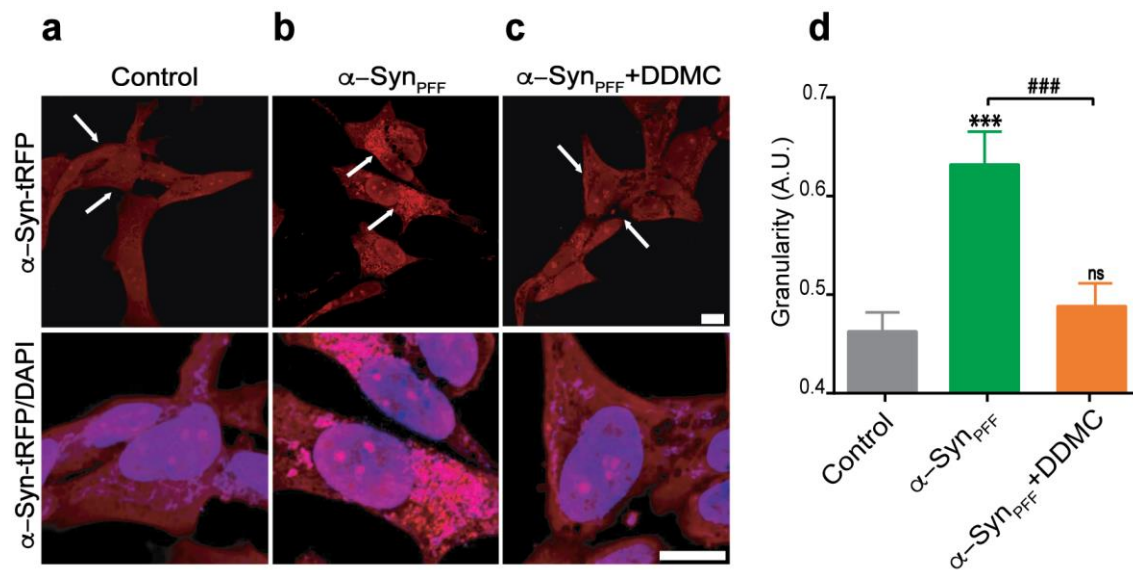
Figure 4. Effect of DDMC on the exogenous α-Syn$_{PFF}$-induced seeding of cytoplasmatic α-Syn. (**a-c**) SH-SY5Y transgenic cell line (Innoprot #P30707-02) expressing α-Syn-tRFP treated with α-Syn$_{PFF}$ or α-Syn$_{PFF}$+DDMC (10 μM). The third column corresponds to an enlargement of the region indicated with arrows. Cells were counterstained with DAPI. (**d**) Granularity was quantified using CellPro-filer 4.2.1. Statistical significance is indicated as: ***p< 0.001 vs. Control; ###p< 0.01 vs α-Syn$_{PFF}$.

3.5-. DDMC inhibits the inflammogenic effects of α-Syn amyloid fibrils

The inflammatory potential of α-Syn depends on the state of protein aggregation. As was previously shown by our group, aggregated species such as α-Syn$_{PFF}$ have strong in-flammogenic properties in microglial cells [52]. These aggregates trigger the release of in-flammatory factors, such as tumor necrosis factor α (TNFα) [52] and glutamate (Glut) [20]. In order to evaluate the ability of DDMC to interfere the release of proinflammatory fac-tors, we treated primary microglial cells with α-Syn$_{PFF}$. After 24 h of treatment, tenfold and eightfold increases in TNFα and Glut release, respectively, were observed (Figure 5a and b). In the presence of DDMC, (α-S$_{PFF}$+DDMC) a significant reduction the release of TNFα and Glut compared to the absence of the novel TC was observed. In addition, we also tested the inflammogenic activity of the remaining fibrils formed in the presence of DDMC, shown in Figure 2c (α-Syn$_{PFF}$:DDMC), by measuring TNFα and Glut release in microglia cells. In order to exclude any effects due to the DDMC itself in the α-Syn$_{PFF}$:DDMC samples, the TC was removed by dialysis before treatment (see Materials and Methods). As expected, α-Syn$_{PFF}$ strongly stimulated the release of TNFα (Figure 5a) and Glut (Figure 5b) after 24 h compared to the control (p< 0.0001). However, when the cultures were exposed to α-Syn$_{PFF}$:DDMC (fibrils formed *in the presence* of DDMC but with no residual DDMC), the release of TNFα and Glut was significantly decreased compared to α-Syn$_{PFF}$, reaching levels comparable to the control condition.
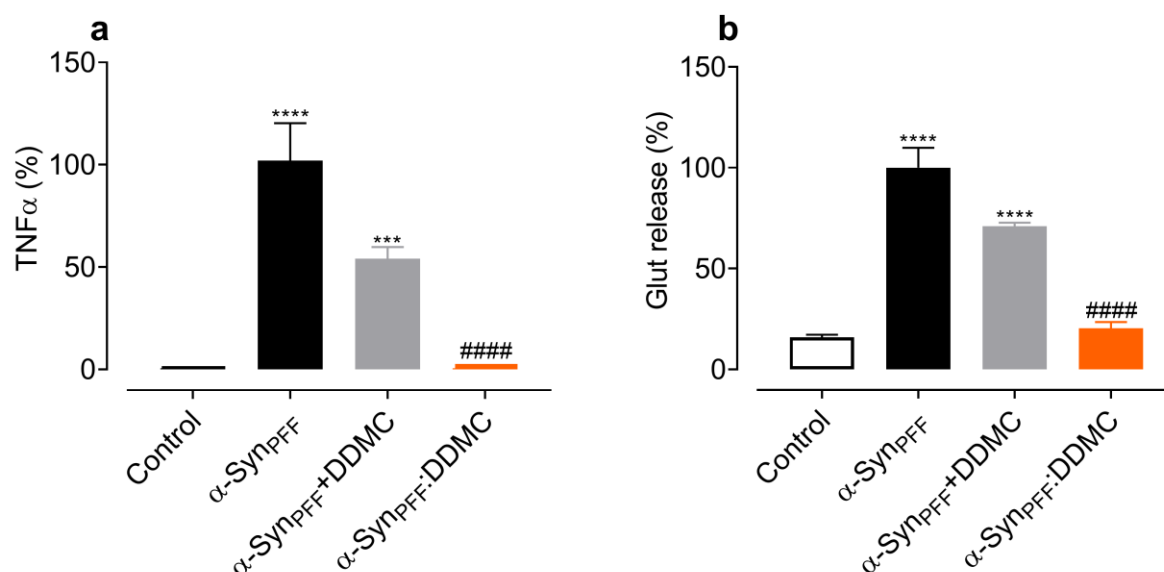
Figure 5. DDMC mitigates the inflammogenic properties of α-Syn amyloid-like fibrils. (**a**) TNFα and (**b**) Glut release from microglial cells for 24 h with i) no treatment (control); ii) α-SynPFF; iii) α-SynPFF with 0.7 µM DDMC (α-SynPFF+DDMC); and iv) α-SynPFF formed in the presence of 10 µM DDMC (α-SynPFF:DDMC) with subsequent dialysis. Bars represent the mean ± S.E.M (n= 8). Statistical significance is indicated as: ***p< 0.001; ****p< 0.001 vs. α-SynPFF; #### p< 0,0001 vs. control; ns—p> 0,05.

4. Discussion

To this day, there is no approved disease-modifying treatment for PD, even less, one that pharmacologically targets neither the formation of α-Syn toxic aggregates nor the inflammatory effect of the aggregated protein. This highlights an unmet need in the development of novel strategies for PD. High-throughput screening systems (HTS) based on the inhibition of α-Syn toxic species provide starting chemical matters for drug discovery processes, and different selection platforms are constantly providing small molecules as hit compounds for PD [18] [28,53] These molecules must be studied in the subsequent steps of drug design pipelines in order to obtain leaders for preclinical and clinical trials. Recently, Braun et al. (2021) identified DMC and the bi-benzimidazole Ro 90-7501 as compounds that prevented α-Syn aggregation at nanomolar concentrations and protected SH-SY5Y cells from αSyn-induced death [18]. Of these, DMC was shown to be the most potent, was effective at a nanomolar range, and could also inhibit α-Syn Ser219 phosphorylation in a murine primary neuron assay [18]. Therefore, this well-known first-generation TC emerged as an exciting candidate for the hit expansion process via chemical modifications.

In the present work, we selected DMC as a starting material for chemical modifications in the hit-to-lead pipeline. Extensive knowledge regarding the properties of TC family ring substituents allowed for the chemical modifications to be carried out in a rational way. For example, the efficient removal of the DMA group in a one-step reaction, as expected, diminished the antibiotic activity of the molecule. The non-antibiotic DDMC described in this work possesses the advantage of overcoming the obstacle poised by antibiotic resistance pressure in long-term administration. Importantly, this novel TC did not alter SH-SY5Y cell viability at a concentration of 50 µM, demonstrating that the new molecule was not toxic in the assays and conditions tested, a property that not all molecules uncovered by HTS possess.

Upon entering the cell, aggregated α-Syn is retained in lysosomes for at least a week [54], and may be proteolytically processed and/or cause lysosomal impairment [55]. However, a small amount of this misfolded α-Syn finds its way through the cytoplasm [56]. Lysosomal dysfunctions have been strongly associated to aggregate-prone protein

deposition, worsening the degradation of abnormal protein aggregates [57]. An increasing number of small molecules have demonstrated the ability to impair lysosomes [57].   Jiang et al. demonstrated that a TC pretreatment could indirectly inhibit autophagy activation in ischemic brain tissues [58]. On the contrary, Lim and Hyun demonstrated that minocycline treatment induced autophagy/lysosome-related gene expression in several tissues and reduced the accumulation of poly-ubiquitinated proteins [59]. The results presented here show that the novel TC DDMC did not affect the number or cellular localization of lysosomes in a cellular model expressing α-Syn-tRFP. These data acquire relevance when considering that lysosomal integrity is an essential point to consider when searching for new small molecules that interfere with α-Syn-induced pathologies.

It is important to notice that the chemical modifications made to DMC were performed in a one-step reaction. This represents an advantage when considering a scaling-up in the synthesis of DDMC for testing in animal models and clinical trials. Moreover, the removal of the DMA group together with the reduction of the hydroxyl in position 12 of ring A increased the efficiency of this molecule at inhibiting the amyloid-like aggregation of α-Syn (Figure 2). Interestingly, this novel derivative displayed not only preserved but also enhanced neuroprotective properties compared to DMC. Accordingly, the ThT and Congo red spectroscopy analysis showed that DDMC strongly inhibited the amyloid-like aggregation of α-Syn at concentrations as low as 10 μM. In order to achieve that level of inhibition, 50 μM of the parental molecule DMC was required. According to our previous results, similar inhibition with doxycycline or CMT-3 was obtained at concentrations of 100 μM [15,20]. This improvement could be useful in future clinical applications.

The data presented herein for DDMC also support our previously proposed amyloid-binding structural motif [14,20]. The fact that specific small molecules had been shown to target the amyloid-like aggregation of different proteins as diverse as PrP, tau, α-synuclein, and Aβ [60] led us to look for a common structural fingerprint that mediates this interaction. Using computational techniques, we uncovered a motif constituted by a proton donor/acceptor pair arrangement attached to a closed ring, arranged in an almost planar configuration at an average distance of 2.6 Å. This arrangement was structurally complementary to the protein backbone in the beta structure [61,62], and we proposed this configuration as responsible for interfering with cross-β formation. In the rational modification of DMC, we preserved this signature (Figure 1, dashed line box). The ability of DDMC to interfere the α-Syn amyloid-like aggregation supports the relevance of this signature in inhibiting the formation of toxic species.

An ideal strategy to prevent PD progression would target not only the formation but also the spread of α-Syn amyloid-like aggregates between close neurons. Growing experimental evidence suggests that the pathological progression of α-Syn pathology is mediated by aggregate-driven or prion-like models of propagation [63,64]. To study this process in cell cultures, Tanik *et al.* developed a model for introducing α-Syn$_{PFF}$ into cells. This widely used model demonstrates the ability of PFFs to act as templates for endogenously expressed α-Syn, which leads to the subsequent formation of insoluble aggregates resembling LBs and Lewy neurites [50,65]. In this way, if DDMC is capable of interfering with this injurious process, it would be useful to not only to avoid the de novo aggregation of native α-Syn but also inhibit the nucleation effect of previously aggregated species. Interestingly, as shown in Figure 3, the seeding ability of pre-aggregated α-Syn was significantly reduced in the presence of DDMC, both *in vitro* as well as in *ex vivo* models. Our data demonstrate that 10 μM of the novel TC turned out to be efficient in reducing the formation of α-Syn$_{PFF}$-induced cytoplasmic inclusions by inhibiting the seeding process. This effect could also be demonstrated in a cell-free model. In our system, α-Syn aggregation followed a typical sigmoidal curve, with a latency time of 16 hs followed by an exponential phase that reached a stationary state around 44 hs (Figure 3a), as was previously described in [17]. In the presence of α-Syn$_{PFF}$, the fast aggregation of the monomeric protein abolished the lag phase. However, in the presence of 10 μM DDMC, α-Syn$_{PFF}$ was inefficient at nucleating new monomers, and the lag phase was restored, reaching 8 h. This suggests that the novel TC "poisons" the seeding reaction, supporting the data observed

in the cell models. In fact, the seeding ability of α-Syn$_{PFF}$ exogenously added to SH-SY5Y-tRFP cells in the presence of DDMC was significantly reduced. Considering that the precise molecular mechanisms underlying the spread and accumulation of α-Syn remain obscure, this data point to the relevance of small molecules with a conserved "amyloid binding motif" for preventing the spread of the pathology and strengthen the position of DDMC as a drug candidate to target not only the formation but also the seeding ability of toxic aggregate α-Syn species.

The well-known ability of TCs to inhibit the release of proinflammatory factors was conserved in DDMC, as depicted in Figure 4, where the inhibition of TNF-α and Glut release was demonstrated. However, we consider the most interesting aspect to be related to the inhibition of the inflammogenic properties of the remanent fibrils formed in the presence of the novel TC. In long-term neuroprotective treatments, the amount of drug is nearly constant; thus, the process shown in Figure 5 could be a simplified recreation of this situation. Therefore, the presence of low concentrations of non-inflammogenic species could contribute synergistically to the neuroprotective process.

Since PD is a multifactorial disorder where protein misfolding yields toxic α-Syn species that spread the pathology, neuroinflammation, and oxidative stress, a cocktail of drugs to target all the different processes should be considered. However, a small multi-target drug could be a better option to minimize the multiple side-effects associated to this kind of treatment. In this way, DDMC arises as a non-toxic, non-antibiotic molecule with the ability to efficiently inhibit α-Syn toxic aggregation seeding and neuroinflammation. The results presented herein lead us to propose this novel TC as a promising drug to be studied further in the drug discovery pipeline.

Author Contributions: Conceptualization, B.F. and R.C.; methodology, R.T.G., F.G.L., D.P., C.L.A., S.B.S., P.B., A.T., C.S., R.M., P.V.L., J.M.B., L.F., B.F., and R.C.; formal analysis, R.T.G., F.G.L., D.P., C.L.A., S.B.S., P.B., and T.A.; investigation, R.T.G., F.G.L., D.P., C.L.A., S.B.S., P.B., A.T., C.S., R.M., P.V.L., C.R., B.S.M., J.M.B., L.F, B.F., and R.C.; writing—original draft preparation, R.T.G., D.P., B.F., and R.C.; writing—review and editing, F.G.L., C.L.A., S.B.S.,R.R.V., P.M., B.F., and R.C.; visualization, R.T.G., F.G.L., R.R.V., P.M., B.F., and R.C.; supervision, B.F. and R.C.; funding acquisition, R.R.V., B.F., and R.C. All authors have read and agreed to the published version of the manuscript.

Institutional Review Board Statement: Not applicable.

Informed Consent Statement: Not applicable.

Data Availability Statement: The datasets generated during the current study are available from the corresponding author upon reasonable request.

Conflicts of Interest: Rosa Mella, Patricia Villacé Lozano, and Clarisa Salado work for Innoprot SL, who developed and commercialized the SH-SY5Y– αS-tRFP cell line used in this study. The other authors declare no competing interest.

References

1. Sapadin, A.N.; Fleischmajer, R. Tetracyclines: nonantibiotic properties and their clinical implications. J Am Acad Dermatol 2006, 54, 258-265, doi:10.1016/j.jaad.2005.10.004.
2. Santa-Cecilia, F.V.; Socias, B.; Ouidja, M.O.; Sepulveda-Diaz, J.E.; Acuna, L.; Silva, R.L.; Michel, P.P.; Del-Bel, E.; Cunha, T.M.; Raisman-Vozari, R. Doxycycline Suppresses Microglial Activation by Inhibiting the p38 MAPK and NF-kB Signaling Pathways. Neurotoxicity research 2016, 29, 447-459, doi:10.1007/s12640-015-9592-2.
3. Yrjanheikki, J.; Keinanen, R.; Pellikka, M.; Hokfelt, T.; Koistinaho, J. Tetracyclines inhibit microglial activation and are neuroprotective in global brain ischemia. Proc Natl Acad Sci U S A 1998, 95, 15769-15774, doi:10.1073/pnas.95.26.15769.
4. Moon, A.; Gil, S.; Gill, S.E.; Chen, P.; Matute-Bello, G. Doxycycline impairs neutrophil migration to the airspaces of the lung in mice exposed to intratracheal lipopolysaccharide. J Inflamm (Lond) 2012, 9, 31, doi:10.1186/1476-9255-9-31.

5. Sultan, S.; Gebara, E.; Toni, N. Doxycycline increases neurogenesis and reduces microglia in the adult hippocampus. Front Neurosci 2013, 7, 131, doi:10.3389/fnins.2013.00131.

6. Noble, W.; Garwood, C.J.; Hanger, D.P. Minocycline as a potential therapeutic agent in neurodegenerative disorders characterised by protein misfolding. Prion 2009, 3, 78-83, doi:10.4161/pri.3.2.8820.

7. Stoilova, T.; Colombo, L.; Forloni, G.; Tagliavini, F.; Salmona, M. A new face for old antibiotics: tetracyclines in treatment of amyloidoses. Journal of medicinal chemistry 2013, 56, 5987-6006, doi:10.1021/jm400161p.

8. Blum, D.; Chtarto, A.; Tenenbaum, L.; Brotchi, J.; Levivier, M. Clinical potential of minocycline for neurodegenerative disorders. Neurobiol Dis 2004, 17, 359-366, doi:10.1016/j.nbd.2004.07.012.

9. Ferreira Junior, N.C.; Dos Santos Pereira, M.; Francis, N.; Ramirez, P.; Martorell, P.; González-Lizarraga, F.; Figadère, B.; Chehin, R.; Del Bel, E.; Raisman-Vozari, R.; et al. The Chemically-Modified Tetracycline COL-3 and Its Parent Compound Doxycycline Prevent Microglial Inflammatory Responses by Reducing Glucose-Mediated Oxidative Stress. Cells 2021, 10, doi:10.3390/cells10082163.

10. Egeberg, A.; Hansen, P.R.; Gislason, G.H.; Thyssen, J.P. Exploring the Association Between Rosacea and Parkinson Disease: A Danish Nationwide Cohort Study. JAMA neurology 2016, 73, 529-534, doi:10.1001/jamaneurol.2016.0022.

11. Du, Y.; Ma, Z.; Lin, S.; Dodel, R.C.; Gao, F.; Bales, K.R.; Triarhou, L.C.; Chernet, E.; Perry, K.W.; Nelson, D.L.; et al. Minocycline prevents nigrostriatal dopaminergic neurodegeneration in the MPTP model of Parkinson's disease. Proc Natl Acad Sci U S A 2001, 98, 14669-14674, doi:10.1073/pnas.251341998.

12. Wu, D.C.; Jackson-Lewis, V.; Vila, M.; Tieu, K.; Teismann, P.; Vadseth, C.; Choi, D.K.; Ischiropoulos, H.; Przedborski, S. Blockade of microglial activation is neuroprotective in the 1-methyl-4-phenyl-1,2,3,6-tetrahydropyridine mouse model of Parkinson disease. J Neurosci 2002, 22, 1763-1771.

13. Investigators, N.N.-P. A pilot clinical trial of creatine and minocycline in early Parkinson disease: 18-month results. Clin Neuropharmacol 2008, 31, 141-150, doi:10.1097/WNF.0b013e3181342f32.

14. Gonzalez-Lizarraga, F.; Socias, S.B.; Avila, C.L.; Torres-Bugeau, C.M.; Barbosa, L.R.; Binolfi, A.; Sepulveda-Diaz, J.E.; Del-Bel, E.; Fernandez, C.O.; Papy-Garcia, D.; et al. Repurposing doxycycline for synucleinopathies: remodelling of alpha-synuclein oligomers towards non-toxic parallel beta-sheet structured species. Scientific reports 2017, 7, 41755, doi:10.1038/srep41755.

15. González-Lizárraga, F.; Ploper, D.; Ávila, C.L.; Socías, S.B.; Dos-Santos-Pereira, M.; Machín, B.; Del-Bel, E.; Michel, P.P.; Pietrasanta, L.I.; Raisman-Vozari, R.; et al. CMT-3 targets different α-synuclein aggregates mitigating their toxic and inflammogenic effects. Scientific reports 2020, 10, 20258, doi:10.1038/s41598-020-76927-0.

16. Fuoco, D. Classification Framework and Chemical Biology of Tetracycline-Structure-Based Drugs. Antibiotics (Basel) 2012, 1, 1-13, doi:10.3390/antibiotics1010001.

17. González-Lizárraga, F.; Socías, S.B.; Ávila, C.L.; Torres-Bugeau, C.M.; Barbosa, L.R.; Binolfi, A.; Sepúlveda-Díaz, J.E.; Del-Bel, E.; Fernandez, C.O.; Papy-Garcia, D.; et al. Repurposing doxycycline for synucleinopathies: remodelling of α-synuclein oligomers towards non-toxic parallel beta-sheet structured species. Scientific reports 2017, 7, 41755, doi:10.1038/srep41755.

18. Braun, A.R.; Liao, E.E.; Horvath, M.; Kalra, P.; Acosta, K.; Young, M.C.; Kochen, N.N.; Lo, C.H.; Brown, R.; Evans, M.D.; et al. Potent inhibitors of toxic alpha-synuclein identified via cellular time-resolved FRET biosensors. NPJ Parkinsons Dis 2021, 7, 52, doi:10.1038/s41531-021-00195-6.

19. Truong, R.; Tang, V.; Grennan, T.; Tan, D.H.S. A systematic review of the impacts of oral tetracycline class antibiotics on antimicrobial resistance in normal human flora. JAC Antimicrob Resist 2022, 4, dlac009, doi:10.1093/jacamr/dlac009.

20. Gonzalez-Lizarraga, F.; Ploper, D.; Avila, C.L.; Socias, S.B.; Dos-Santos-Pereira, M.; Machin, B.; Del-Bel, E.; Michel, P.P.; Pietrasanta, L.I; Raisman-Vozari, R.; et al. CMT-3 targets different alpha-synuclein aggregates mitigating their toxic and inflammogenic effects. Scientific reports 2020, 10, 20258, doi:10.1038/s41598-020-76927-0.

21. Hoyer, W.; Antony, T.; Cherny, D.; Heim, G.; Jovin, T.M.; Subramaniam, V. Dependence of alpha-synuclein aggregate morphology on solution conditions. J Mol Biol 2002, 322, 383-393, doi:S0022283602007751 [pii].

22. Members of the, S.F.M.A.C. Comite de l'Antibiogramme de la Societe Francaise de Microbiologie report 2003. Int J Antimicrob Agents 2003, 21, 364-391, doi:10.1016/s0924-8579(03)00021-9.

23. LeVine, H., 3rd. Thioflavine T interaction with synthetic Alzheimer's disease beta-amyloid peptides: detection of amyloid aggregation in solution. Protein Sci 1993, 2, 404-410.

24. Klunk, W.E.; Jacob, R.F.; Mason, R.P. Quantifying amyloid by congo red spectral shift assay. Methods Enzymol 1999, 309, 285-305.

25. LeVine, H., 3rd. Stopped-flow kinetics reveal multiple phases of thioflavin T binding to Alzheimer beta (1-40) amyloid fibrils. Arch Biochem Biophys 1997, 342, 306-316, doi:10.1006/abbi.1997.0137.

26. Lau, A.; So, R.W.L.; Lau, H.H.C.; Sang, J.C.; Ruiz-Riquelme, A.; Fleck, S.C.; Stuart, E.; Menon, S.; Visanji, N.P.; Meisl, G.; et al. alpha-Synuclein strains target distinct brain regions and cell types. Nat Neurosci 2020, 23, 21-31, doi:10.1038/s41593-019-0541-x.

27. Stirling, D.R.; Swain-Bowden, M.J.; Lucas, A.M.; Carpenter, A.E.; Cimini, B.A.; Goodman, A. CellProfiler 4: improvements in speed, utility and usability. BMC Bioinformatics 2021, 22, 433, doi:10.1186/s12859-021-04344-9.

28. Svanbergsson, A.; Ek, F.; Martinsson, I.; Rodo, J.; Liu, D.; Brandi, E.; Haikal, C.; Torres-Garcia, L.; Li, W.; Gouras, G.; et al. FRET-Based Screening Identifies p38 MAPK and PKC Inhibition as Targets for Prevention of Seeded alpha-Synuclein Aggregation. Neurotherapeutics : the journal of the American Society for Experimental NeuroTherapeutics 2021, 18, 1692-1709, doi:10.1007/s13311-021-01070-1.

29. Angusti, A.H., S. T.; Jiang, X. S.; Komatsu, H.; Konishi, Y.; Kubo, T.; Lertvorachon, J.; Roman, G. Tetracyclines and Their Use as Calpain Inhibitors. September 9, 2005.

30.   Abato, P.A., H.; Berniac, J.; Bowser, T.; Chen, J.; Grier, M.; Honeyman, L. Tetracyclines 10-Substituees Et Leurs Procedes D'utilisation. February 1, 2007.

31.   Sucholeiki, I. Compounds and Methods for the Treatment of Pain and Other Diseases. September 22, 2011.

32.   Socias, S.B.; Gonzalez-Lizarraga, F.; Avila, C.L.; Vera, C.; Acuna, L.; Sepulveda-Diaz, J.E.; Del-Bel, E.; Raisman-Vozari, R.; Chehin, R.N. Exploiting the therapeutic potential of ready-to-use drugs: Repurposing antibiotics against amyloid aggregation in neurodegenerative diseases. Prog Neurobiol 2018, 162, 17-36, doi:10.1016/j.pneurobio.2017.12.002.

33.   Edan, R.A.; Luqmani, Y.A.; Masocha, W. COL-3, a chemically modified tetracycline, inhibits lipopolysaccharide-induced microglia activation and cytokine expression in the brain. PLoS One 2013, 8, e57827, doi:10.1371/journal.pone.0057827.

34.   Sarkar, S.; Li, Y.; Mirzaei, R.; Rawji, K.S.; Poon, C.C.; Wang, J.; Kumar, M.; Bose, P.; Yong, V.W. Demeclocycline Reduces the Growth of Human Brain Tumor-Initiating Cells: Direct Activity and Through Monocytes. Front Immunol 2020, 11, 272, doi:10.3389/fimmu.2020.00272.

35.   Mosmann, T. Rapid colorimetric assay for cellular growth and survival: application to proliferation and cytotoxicity assays. J Immunol Methods 1983, 65, 55-63.

36.   Fleming, A.; Bourdenx, M.; Fujimaki, M.; Karabiyik, C.; Krause, G.J.; Lopez, A.; Martin-Segura, A.; Puri, C.; Scrivo, A.; Skidmore, J.; et al. The different autophagy degradation pathways and neurodegeneration. Neuron 2022, 110, 935-966, doi:10.1016/j.neuron.2022.01.017.

37.   Finkbeiner, S. The Autophagy Lysosomal Pathway and Neurodegeneration. Cold Spring Harb Perspect Biol 2020, 12, doi:10.1101/cshperspect.a033993.

38.   Klionsky, D.J.; Abdelmohsen, K.; Abe, A.; Abedin, M.J.; Abeliovich, H.; Acevedo Arozena, A.; Adachi, H.; Adams, C.M.; Adams, P.D.; Adeli, K.; et al. Guidelines for the use and interpretation of assays for monitoring autophagy (3rd edition). Autophagy 2016, 12, 1-222, doi:10.1080/15548627.2015.1100356.

39.   Kuo, S.H.; Tasset, I.; Cheng, M.M.; Diaz, A.; Pan, M.K.; Lieberman, O.J.; Hutten, S.J.; Alcalay, R.N.; Kim, S.; Ximenez-Embun, P.; et al. Mutant glucocerebrosidase impairs alpha-synuclein degradation by blockade of chaperone-mediated autophagy. Sci Adv 2022, 8, eabm6393, doi:10.1126/sciadv.abm6393.

40.   Vilar, M.; Chou, H.T.; Luhrs, T.; Maji, S.K.; Riek-Loher, D.; Verel, R.; Manning, G.; Stahlberg, H.; Riek, R. The fold of alpha-synuclein fibrils. Proc Natl Acad Sci U S A 2008, 105, 8637-8642, doi:10.1073/pnas.0712179105.

41.   Biancalana, M.; Koide, S. Molecular mechanism of Thioflavin-T binding to amyloid fibrils. Biochim Biophys Acta 2010, 1804, 1405-1412, doi:10.1016/j.bbapap.2010.04.001.

42.   Groenning, M. Binding mode of Thioflavin T and other molecular probes in the context of amyloid fibrils-current status. J Chem Biol 2010, 3, 1-18, doi:10.1007/s12154-009-0027-5.

43.   Espargaró, A.; Llabrés, S.; Saupe, S.J.; Curutchet, C.; Luque, F.J.; Sabaté, R. On the Binding of Congo Red to Amyloid Fibrils. Angew Chem Int Ed Engl 2020, 59, 8104-8107, doi:10.1002/anie.201916630.

44.   Tornquist, M.; Michaels, T.C.T.; Sanagavarapu, K.; Yang, X.; Meisl, G.; Cohen, S.I.A.; Knowles, T.P.J.; Linse, S. Secondary nucleation in amyloid formation. Chem Commun (Camb) 2018, 54, 8667-8684, doi:10.1039/c8cc02204f.

45.   Schweighauser, M.; Shi, Y.; Tarutani, A.; Kametani, F.; Murzin, A.G.; Ghetti, B.; Matsubara, T.; Tomita, T.; Ando, T.; Hasegawa, K.; et al. Structures of alpha-synuclein filaments from multiple system atrophy. Nature 2020, 585, 464-469, doi:10.1038/s41586-020-2317-6.

46.   Luk, K.C.; Kehm, V.; Carroll, J.; Zhang, B.; O'Brien, P.; Trojanowski, J.Q.; Lee, V.M. Pathological alpha-synuclein transmission initiates Parkinson-like neurodegeneration in nontransgenic mice. Science 2012, 338, 949-953, doi:10.1126/science.1227157.

47.   Luk, K.C.; Kehm, V.M.; Zhang, B.; O'Brien, P.; Trojanowski, J.Q.; Lee, V.M. Intracerebral inoculation of pathological alpha-synuclein initiates a rapidly progressive neurodegenerative alpha-synucleinopathy in mice. J Exp Med 2012, 209, 975-986, doi:10.1084/jem.20112457.

48.   Masuda-Suzukake, M.; Nonaka, T.; Hosokawa, M.; Oikawa, T.; Arai, T.; Akiyama, H.; Mann, D.M.; Hasegawa, M. Prion-like spreading of pathological alpha-synuclein in brain. Brain 2013, 136, 1128-1138, doi:10.1093/brain/awt037.

49.   Luk, K.C.; Song, C.; O'Brien, P.; Stieber, A.; Branch, J.R.; Brunden, K.R.; Trojanowski, J.Q.; Lee, V.M. Exogenous alpha-synuclein fibrils seed the formation of Lewy body-like intracellular inclusions in cultured cells. Proc Natl Acad Sci U S A 2009, 106, 20051-20056, doi:10.1073/pnas.0908005106.

50.   Tanik, S.A.; Schultheiss, C.E.; Volpicelli-Daley, L.A.; Brunden, K.R.; Lee, V.M. Lewy body-like alpha-synuclein aggregates resist degradation and impair macroautophagy. J Biol Chem 2013, 288, 15194-15210, doi:10.1074/jbc.M113.457408.

51.   Volpicelli-Daley, L.A.; Luk, K.C.; Lee, V.M. Addition of exogenous alpha-synuclein preformed fibrils to primary neuronal cultures to seed recruitment of endogenous alpha-synuclein to Lewy body and Lewy neurite-like aggregates. Nat Protoc 2014, 9, 2135-2146, doi:10.1038/nprot.2014.143.

52.   Acuña, L.; Hamadat, S.; Corbalán, N.S.; González-Lizárraga, F.; Dos-Santos-Pereira, M.; Rocca, J.; Díaz, J.S.; Del-Bel, E.; Papy-García, D.; Chehín, R.N.; et al. Rifampicin and Its Derivative Rifampicin Quinone Reduce Microglial Inflammatory Responses and Neurodegeneration Induced In Vitro by α-Synuclein Fibrillary Aggregates. Cells 2019, 8, doi:10.3390/cells8080776.

53.   Kurnik, M.; Sahin, C.; Andersen, C.B.; Lorenzen, N.; Giehm, L.; Mohammad-Beigi, H.; Jessen, C.M.; Pedersen, J.S.; Christiansen, G.; Petersen, S.V.; et al. Potent alpha-Synuclein Aggregation Inhibitors, Identified by High-Throughput Screening, Mainly Target the Monomeric State. Cell Chem Biol 2018, 25, 1389-1402 e1389, doi:10.1016/j.chembiol.2018.08.005.

54.   Karpowicz, R.J., Jr.; Haney, C.M.; Mihaila, T.S.; Sandler, R.M.; Petersson, E.J.; Lee, V.M. Selective imaging of internalized proteopathic alpha-synuclein seeds in primary neurons reveals mechanistic insight into transmission of synucleinopathies. J Biol Chem 2017, 292, 13482-13497, doi:10.1074/jbc.M117.780296.

55. Jiang, P.; Gan, M.; Yen, S.H.; McLean, P.J.; Dickson, D.W. Impaired endo-lysosomal membrane integrity accelerates the seeding progression of alpha-synuclein aggregates. Scientific reports 2017, 7, 7690, doi:10.1038/s41598-017-08149-w.

56. Henderson, M.X.; Trojanowski, J.Q.; Lee, V.M. alpha-Synuclein pathology in Parkinson's disease and related alpha-synucleinopathies. Neurosci Lett 2019, 709, 134316, doi:10.1016/j.neulet.2019.134316.

57. Whitmarsh-Everiss, T.; Laraia, L. Small molecule probes for targeting autophagy. Nat Chem Biol 2021, 17, 653-664, doi:10.1038/s41589-021-00768-9.

58. Jiang, Y.; Zhu, J.; Wu, L.; Xu, G.; Dai, J.; Liu, X. Tetracycline inhibits local inflammation induced by cerebral ischemia via modulating autophagy. PLoS One 2012, 7, e48672, doi:10.1371/journal.pone.0048672.

59. Lim, J.J.; Hyun, S. Minocycline treatment improves proteostasis during Drosophila aging via autophagy mediated by FOXO and Hsp70. Biomed Pharmacother 2022, 149, 112803, doi:10.1016/j.biopha.2022.112803.

60. Giorgetti, S.; Raimondi, S.; Pagano, K.; Relini, A.; Bucciantini, M.; Corazza, A.; Fogolari, F.; Codutti, L.; Salmona, M.; Mangione, P.; et al. Effect of tetracyclines on the dynamics of formation and destructuration of beta2-microglobulin amyloid fibrils. J Biol Chem 2011, 286, 2121-2131, doi:10.1074/jbc.M110.178376.

61. Sunde, M.; Serpell, L.C.; Bartlam, M.; Fraser, P.E.; Pepys, M.B.; Blake, C.C. Common core structure of amyloid fibrils by synchrotron X-ray diffraction. J Mol Biol 1997, 273, 729-739, doi:10.1006/jmbi.1997.1348.

62. Jahn, T.R.; Radford, S.E. The Yin and Yang of protein folding. Febs J 2005, 272, 5962-5970.

63. Chung, H.K.; Ho, H.A.; Perez-Acuna, D.; Lee, S.J. Modeling alpha-Synuclein Propagation with Preformed Fibril Injections. J Mov Disord 2020, 13, 77-79, doi:10.14802/jmd.19046.e.

64. Brundin, P.; Melki, R. Prying into the Prion Hypothesis for Parkinson's Disease. J Neurosci 2017, 37, 9808-9818, doi:10.1523/JNEUROSCI.1788-16.2017.

65. Vasili, E.; Dominguez-Meijide, A.; Flores-Leon, M.; Al-Azzani, M.; Kanellidi, A.; Melki, R.; Stefanis, L.; Outeiro, T.F. Endogenous Levels of Alpha-Synuclein Modulate Seeding and Aggregation in Cultured Cells. Mol Neurobiol 2022, 59, 1273-1284, doi:10.1007/s12035-021-02713-2.